Desalination and Water Treatment
www.deswater.com
doi: 10.5004/dwt.2020.26097

198 (2020) 211–223
September

Tertiary treatment of pulp and paper mill wastewater by iron–carbon micro-electrolysis coupled with H_2O_2

Xia Shao[a], Kang Du[b,*]

[a]*Beijing Municipal Research Institute of Environmental Protection, Beijing 100037, China, email: 372729068@qq.com (X. Shao)*
[b]*China Energy Conservation and Environmental Protection Group, China International Engineering Consulting Corporation Environmental Investment Management Co., Ltd., Beijing 100034, China, Tel./Fax: +86 10 84665487; email: lang.dk@163.com (K. Du)*

Received 21 December 2019; Accepted 7 May 2020

ABSTRACT

The conventional biological treatment of pulp and paper mill wastewater may not be enough to satisfy the discharge limits, more effective processes such as advanced oxidation technologies may be used as advanced treatments for the removal of color and refractory contaminants. In this study, biologically treated effluent from pulp and paper mill (BTEPM) has been examined by iron–carbon micro-electrolysis coupled with H_2O_2 (ICME-H_2O_2). Under the optimal treatment conditions (Fe/C = 1:2.5, pH = 2.5, 100 min reaction, 9 mmol/L H_2O_2 added in three aliquots), the chemical oxygen demand (COD) removal efficiency attained 81% which is much more efficient than ICME without H_2O_2 under its optimal experimental conditions (42%). In addition, the initial biodegradability of BTEPM, as shown by BOD_5/COD ratio, can be enhanced after treatment. The morphology and content of iron and the evolution of H_2O_2 content in the system under the optimal operating parameters were studied.

Keywords: Biologically treated effluent from pulp and paper mill; ICME-H_2O_2; Hydrogen peroxide; Kinetic analysis

1. Introduction

Pulp and paper industry is a large producer of wastewater, which has caused serious environmental pollution. After the treatment by traditional primary and secondary treatment methods, suspended substances, and biodegradable soluble pollutants in pulping and papermaking wastewater which has complex water quality, high chromaticity, and poor biodegradability can be removed to a large extent, and the chemical oxygen demand (COD), suspended substances, and color of effluent decrease greatly. However, the treatment efficiency of soluble substances (such as lignin and its degradable debris) which are difficult to biodegrade is not high, and the decolorization effect is also poor, and the advanced treatment of papermaking wastewater has gradually become a highly concerned environmental treatment project [1].

Fenton oxidation has been used in wastewater treatment and has achieved ideal results [2,3], and Fenton oxidation process can also be applied to advanced treatment of papermaking wastewater. Under acidic conditions, hydrogen peroxide is catalyzed by Fe^{2+} ions to produce $^{\bullet}OH$, which can remove pollutants. Although the removal efficiency of COD by this method is high, it is difficult to popularize and apply because of the high cost of pharmaceuticals, a large amount of acid and alkali consumed in regulating pH step, and the high running cost. It is necessary to seek an efficient and economical process to meet the treatment needs [4–8].

Iron–carbon micro-electrolysis (ICME) is based on battery reaction in electrochemistry [9]. A large number of corrosive micro-batteries will be formed when iron–carbon filler is in an electrolyte solution. When iron is corroded as an anode and consumed by electrode reaction, nascent Fe^{2+} will be formed, which have high reactivity [10]. The Fenton

* Corresponding author.

reagent can be formed by adding H_2O_2 to ICME, which can effectively treat the biologically treated effluent from pulp and paper mill (BTEPM) [11]. Chanworrawoot and Hunsom [12] presented a complete study on the electrochemical treatment of effluent from the digestor of pulp and paper mill. The pH of effluent is 11.87, and the concentration of NaCl is 2 g/L. After electrolysis for 3 h at 2.53 mA/cm^2, the removal efficiency of color, biochemical oxygen demand (BOD), and COD can reach 98%, 98%, and 97%, respectively, and the energy consumption is 70 kWh/m^3. Thus, the electrochemical method could be considered as a promising and efficient emergent technology to treat this kind of industrial effluent.

Based on the above analysis, a treatment process of ICME was used to deal with BTEPM, and the effect of adding hydrogen peroxide on COD removal by ICME was studied. The optimum conditions for treatment of BTEPM by ICME and iron–carbon micro-electrolysis coupled with hydrogen peroxide (ICME-H_2O_2) were studied, and the mechanism of COD removal by ICME-H_2O_2 was analyzed, which could provide reference for advanced treatment of papermaking wastewater.

2. Materials and methods

2.1. Characteristics of BTEPM

The wastewater sample was taken from a pulp and paper mill in Jiaxing, Zhejiang Province. It uses chemical pulping and elemental chlorine free bleaching processes. The main raw materials for pulping are natural wood pulp, domestic waste paper, imported waste paper, rosin, aluminum sulfate, and chemical additives, and the like. The generated papermaking wastewater first passed through the primary sedimentation tank to remove some suspended substances. Then it passed through the anaerobic reactor, the A/O system and the secondary sedimentation tank for biological treatment, and the effluent is BTEPM. The properties of BTEPM are listed in Table 1, the COD is much higher than BOD_5, which indicates that BTEPM contains a lot of organics that are difficult to be biodegraded. Before use, the BTEPM have not been pre-treated and were kept in the refrigerator to preserve their characteristics.

2.2. Materials and chemicals

The materials used in the experiment were iron scrap with sieved sizes of 20–50 mesh and columnar activated carbon with diameter of 1.5 mm. As oily contaminants and oxide film may cover the surface of iron scrap, and activated carbon can absorb some organic compounds in water, which will affect the contact between iron and carbon. In order to avoid the influence of impurities, the materials were pretreated before the experiment. The iron scrap was placed in a beaker containing 1 mol/L NaOH and heated in a water bath at 50°C for 30 min. After washing, it was immersed in 10% dilute sulfuric acid for 15 min, washed with distilled water, and dried for later use. The activated carbon was immersed in the test wastewater for 48 h, and the water was changed every 24 h until the adsorption was saturated [13].

Table 1
Characteristics of the BTEPM

Parameter	Values
pH	6.3–7.5
SS (mg/L)	35–47
COD (mg/L)	189–240
BOD_5 (mg/L)	13–17
Color (mgPt/L)	70–90

All chemical reagents (chemical pure) used in this study, including ammonium chloride (NH_4Cl), potassium dihydrogen phosphate (KH_2PO_4), hydrogen peroxide (H_2O_2), iron (II) sulfate heptahydrate ($FeSO_4{\cdot}7H_2O$), polyacrylamide (PAM), hydrochloric acid (HCl), sodium hydroxide (NaOH), and sulfuric acid (H_2SO_4) were purchased from Sinopharm Group Chemical Reagent Co., Ltd., in China. Distilled water was used for dilution of all solutions.

2.3. Analytical methods

COD was determined using the potassium dichromate method and BOD_5 were tested by biochemical oxygen demand analyzer (Lovibond ET99724N, Germany). Total organic carbon (TOC) was determined by TOC tester (TOC-V_{CPN}, Shimadzu, Japan). The color was determined by platinum–cobalt colorimetry (ISO 7887-1985, water quality – examination and determination of color). The content of Fe^{2+} and total iron were determined by phenanthroline spectrophotometry [14]. The content of Fe^{3+} was derived from the total iron content minus the ferrous iron content; the pH was measured by pH meter (HACH HQ40D PHC301, Loveland, America); the content of H_2O_2 was determined by potassium titanium oxalate spectrophotometry [15]. The ultraviolet-visible spectroscopy of wastewater were recorded on a Shimadzu UV-1800 spectrophotometer in a 1 cm quartz cuvette and scanned from 200 to 700 nm with 1 nm wavelength interval.

2.4. Experimental methods

The studied treatment was formed in a beaker with a volume of 2 L and the horizontal sedimentation tank with a volume of 2.5 L. An aeration pump (BT300M) was used for aeration with sand core aeration diffuser at the bottom of the treating tank. Add micro-electrolytic filler into the beaker. The micro-electrolytic filler was composed of activated carbon and iron scrap according to a certain mass ratio. The sand core aeration diffuser was embedded in the filler and connected with the aeration pump to fully agitate the BTEPM, which can effectively prevent the filler from hardening and can also make the Fe^{2+} generated by micro-electrolysis more evenly diffused into the BTEPM to improve the reaction rate.

Before the reactor operation, the pH value of the solution was adjusted to the desired range using 10% sulfuric acid. After a certain time of reaction, we adjusted the pH of the BTEPM to 7–8 and added 1 mL/L 1‰ polyacrylamide solution (PAM). Then the solution was stirred with 300 rpm for 3 min and 80 rpm for 15 min. Finally, we took the supernatant of the sedimentation tank to measure COD,

calculate the removal efficiency and judge the treatment effect.

In the ICME-H_2O_2, a certain amount of 30% H_2O_2 was added after the pH was adjusted without changing the amount of iron scrap and the iron–carbon ratio. The subsequent operation steps were same as the above experimental methods. The experimental device of combined treatment system is shown in Fig. 1.

2.5. Orthogonal tests design

Orthogonal test is a method to study multi-factor and multi-level test. It selects representative points from comprehensive experiments for testing. By using this method, the best experimental conditions can be found quickly, which greatly saves time and reduces workload [16]. The iron dosage (*A*), the ratio of Fe/C (*B*), pH (*C*), and reaction time (*D*) have a great influence on the performance of ICME. These parameters were set as four factors in orthogonal test of ICME. Details of these four-factors and three-levels orthogonal tests are shown in Table 2. The choice of three levels of these four factors is based on the results of parameter optimization experiments. Nine orthogonal tests were designed as Table S1.

The pH (*A*), the concentration of H_2O_2 (*B*), and reaction time (*C*) have a great influence on the performance of ICME-H_2O_2. These parameters were set as three factors in orthogonal test of ICME-H_2O_2. Details of these three-factors and three-levels orthogonal tests were shown in Table 3. The choice of three levels of these three factors is based on the results of parameter optimization experiments. Nine orthogonal tests are designed as Table S2.

In this study, the range analysis method was used to determine the sensitivity of each factor to the results in orthogonal test. According to orthogonal test of Lin et al. [17], some modifications were made and the following formula was obtained:

$$\bar{K}_{X,y} = \frac{\left(E_{X,y,1} + E_{X,y,2} + E_{X,y,3}\right)}{3} \tag{1}$$

$$R_{0X} = \max \bar{K}_{X,y} \tag{2}$$

$$R_{1X} = \min \bar{K}_{X,y} \tag{3}$$

$$R_X = R_{0X} - R_{1X} \tag{4}$$

where $E_{X,y}$ is the COD removal efficiency corresponding to factor X at the y level ($E_{X,y}$ has three values, expressed as $E_{X,y,1}$, $E_{X,y,2}$, $E_{X,y,3}$), $\bar{E}_{X,y}$ is the average of the removal efficiency corresponding to factor X at the y level, R_X is the extreme difference under the X factor, which refers to the difference between the maximum and minimum values of the average removal efficiency of the X factor at each level. R_X reflects the magnitude of the change in removal efficiency when factor X changes. The larger the R_X is, the greater the influence of this factor on the treatment effect. So according to the value of R_X, we can judge the importance of this factor.

2.6. Degradation kinetics of ICME-H_2O_2

In order to study the mechanism of COD removal, the curve of COD concentration with time was fitted with the following kinetic models [18,19]:

Zero-order reaction kinetics:

$$C_t = C_0 - k_0 t \tag{5}$$

Double exponential model:

$$\frac{C_t}{C_0} = a_1 e^{-k_{1,1}t} + a_2 e^{-k_{1,2}t} \tag{6}$$

Second-order reaction kinetics:

$$\frac{1}{C_t} = \frac{1}{C_0} + k_2 t \tag{7}$$

where C_t was the COD concentration (mg/L) at time t, C_0 was the COD concentration (mg/L) at time zero, t was the

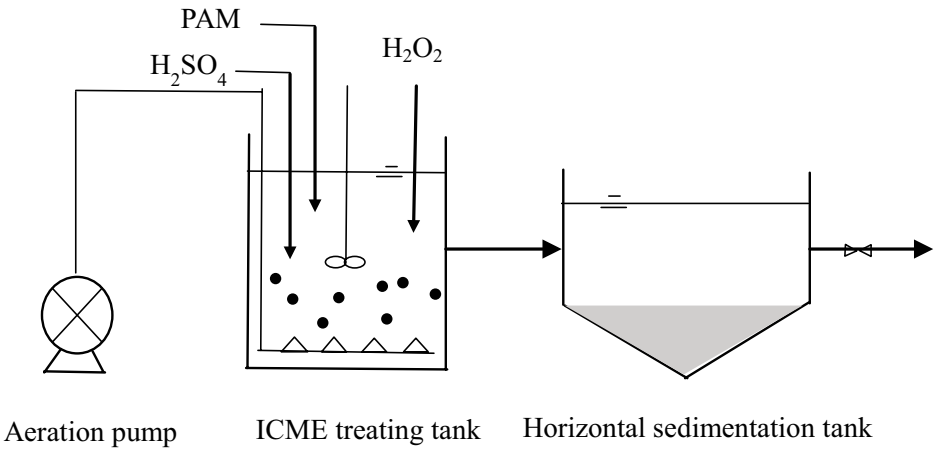

Fig. 1. Experimental device of iron–carbon micro-electrolysis (ICME) system.

Table 2
Parameters levels definition for orthogonal test of ICME system

Level	Iron scrap (g/L) (*A*)	Fe/C ratio (*B*)	pH (*C*)	RT (min) (*D*)
1	15	1:1.5	2.5	80
2	20	1:2	3	90
3	25	1:2.5	3.5	100

time (min), k_0 was the zero-order rate constant (mg/L/min), a_1 and a_2 represent fraction coefficients, $k_{1,1}$ and $k_{1,2}$ are apparent rate constants (1/min) for the first type and second type of COD degradation, and k_2 was the second-order rate constant (1/min).

3. Results and discussion

3.1. Optimum parameters for ICME process

3.1.1. Effect of iron dosage on COD removal efficiency

The influence of the iron dosage on the COD removal efficiency was evaluated and the results are displayed in Fig. 2a. From the 2a, it can be seen that the process is divided into two stages. First, with the increase of iron dosage, the removal efficiency increased significantly. The removal efficiency increased from 11% to 30% when iron dosage from 10 to 20 g/L. Then, with the increase of dosage, the removal efficiency remained nearly constant.

When the Fe/C remains unchanged, increasing the amount of iron scrap can increase the number of galvanic cells, and then enhance the micro-electrolysis reaction. The nascent H^+ and Fe^{2+} produced by the ICME have strong chemical activity in acidic environment, mainly reflected in the reducibility, which can destroy some chromogenic groups and increase the COD removal efficiency [20].

When the dosage of iron exceeds 20 g/L, the removal efficiency of COD tends to be gentle. The main reason is that the number of iron–carbon galvanic cells in the system has reached the saturation state at this time. Continuing to increase the amount of iron scrap can increase the number of galvanic cells, but it will also cause excess iron, and will react with H^+ in water, which will hinder the micro-electrolysis reaction [21]. Therefore, the removal efficiency of COD will not change or even decreased slightly. Considering the economic cost and treatment effect, the iron scrap dosage is 20 g/L.

3.1.2. Effect of Fe/C on COD removal efficiency

According to Fig. 2b, as the Fe/C gradually decreases, the COD removal efficiency first rises, reaches a maximum value, then gradually decreases and tends to be stable. The highest COD removal efficiency was 32%.

When the dosage of iron scrap is 20 g/L, the content of iron increases with the increase of the ratio of Fe/C, the excess anode (Fe) will participate in the displacement reaction with H^+, which will hinder the micro-electrolytic reaction [22]. At the same time, the content of carbon decreases with the increase of the ratio of Fe/C, so the content of cathode (*C*) decreases, which leads to the reduction of the galvanic cells. The galvanic cells constitute micro-electrolysis reaction, so the removal efficiency of COD decreases. When the ratio of Fe/C is 4:1, the removal efficiency of COD is less than 20%. When the ratio of Fe/C decreases, the content of iron decreases, and the content of carbon increases, which reduces the influence of excessive anode, increases the contact area between cathode and anode, increases the number of galvanic cells, and leads to the increase of COD removal efficiency.

When Fe/C is 1:2, the COD removal efficiency is the highest, indicating that the conditions in the system are most suitable at this time, and the number of galvanic cells is the largest. Because the anode (Fe) mainly participates in the electrode reaction, when the amount of activated carbon is increased, excess activated carbon does not participate in the electrode reaction, it will only increase the cost. Therefore, the best ratio of Fe/C was chosen to be 1:2.

Table 3
Parameters levels definition for orthogonal test of ICME-H_2O_2 system

Level	pH (*A*)	H_2O_2 (mmol/L) (*B*)	RT (min) (*C*)
1	2.5	9	80
2	3	10	90
3	3.5	11	100

3.1.3. Effect of pH on COD removal efficiency

As can be shown from Fig. 2c, as the pH value decreases, the COD removal efficiency gradually increases. When the pH value is 3 and 2, the COD removal efficiency corresponds to 35% and 36%, respectively. Without pH adjustment of raw water, COD is only removed in a small amount. The BTEPM can obtain a higher COD removal efficiency at a lower pH, mainly because lowering the pH of the BTEPM can significantly increase the redox potential of the mixed system, and the formed iron–carbon galvanic cells can obtain a higher electromotive force and the micro-electrolytic reaction is more effective. In addition, a lower pH value can effectively protect the galvanic cells electrode and prevent electrode polarization and passivation [23]. However, too low pH does not result in higher removal efficiency. The reason is that the pH is too low, and a large amount of H^+ will react with the anode (Fe). Although the galvanic cells can obtain a higher electromotive force, the generated H_2 will hinder the contact between the anode and cathode, leading to a decrease in reaction efficiency [24]. In addition, obtaining a lower pH requires a large amount of acid to adjust, and the operating cost will also increase.

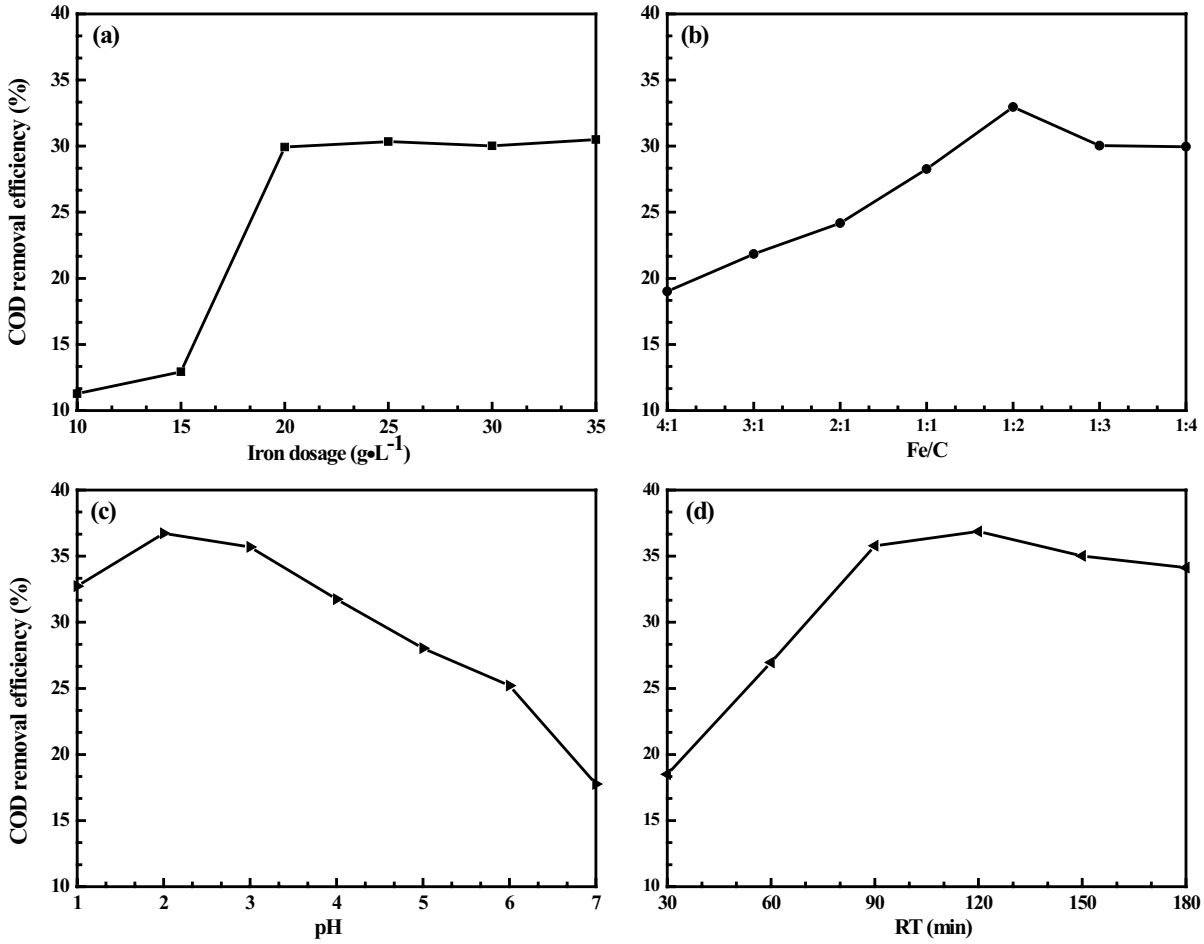

Fig. 2. Effects of operational parameters on COD removal efficiency using ICME. (a) Effect of iron dosage (Fe/C = 1:1, RT = 120 min, and pH = 3), (b) effect of Fe/C (iron dosage = 20 g/L, RT = 120 min, and pH = 3), (c) effect of pH (iron dosage = 20 g/L, Fe/C = 1:1, and RT = 120 min), and (d) effect of reaction time (iron dosage = 20 g/L, Fe/C = 1:1, and pH = 3).

Therefore, on the basis of comprehensive consideration of treatment cost and treatment effect, the optimal pH is 3.

3.1.4. Effect of reaction time on COD removal efficiency

COD removal efficiency under different reaction times are shown in Fig. 2d. With the increase of reaction time, COD removal efficiency gradually rises to the highest point of 35%, and then remains unchanged, even has the trend of slow fluctuation and decline. The reason is that with the increase of reaction time, the micro-electrolysis reaction is more complete, and the number of nascent H^+, nascent Fe^{2+}, Fe^{3+} produced by electrode reaction increases, which has a great promotion on the subsequent coagulation and sedimentation stage; secondly, the extension of reaction time can more effectively decompose organic compounds and some toxic substances. When the COD removal efficiency rises to the highest point, the pH of the system will gradually increase due to the reaction, and a small amount of flocculant will be produced. When it adheres to the electrode, the electrode will be passivated, which will hinder the contact between the cathode and the anode and inhibit the micro-electrolysis reaction [25]. In addition, it can be seen from the graph that excessive reaction time does not increase the COD removal efficiency, but increases the cost of the reaction structure. When the reaction time is 90 min, the removal efficiency can reach 35%. The reaction time was chosen to be 90 min based on the cost and COD removal efficiency.

3.1.5. Orthogonal test

In order to determine the optimal process conditions for the ICME system, orthogonal tests were carried out and the results are shown in Table S1. The results of orthogonal test are analyzed by range analysis method, and the results are shown in Table S2. According to the value of R_X, the order of the influence of these factors on the treatment effect is as follows: Fe/C ratio > pH value > iron dosage > reaction time. The optimum combination is iron dosage of 25 g/L, Fe/C ratio of 1:2.5, pH of 2.5, and reaction time of 90 min.

3.2. Optimum parameters for ICME-H_2O_2 process

The advanced treatment of papermaking wastewater by ICME-H_2O_2 was studied without changing the iron dosage and the ratio of Fe/C.

3.2.1. Effect of pH on COD removal efficiency

As can be seen from Fig. 3a, when the initial value of pH is 2, COD removal efficiency is 68%, when the pH is 3, the removal efficiency is the highest, 77%. With the gradual increase of pH, COD removal efficiency shows a significant downward trend, the overall curve shows a trend of low at both ends and high in the middle.

Under the ICME-H_2O_2 process, Fe^{2+} generated by micro-electrolysis and H_2O_2 constitute Fenton system for oxidation and decomposition of organic matter in actual wastewater. Therefore, pH will not only affect the production of Fe^{2+} in the process of micro-electrolysis, but also affect the production and activity of •OH in the Fenton process [26]. As mentioned in the foregoing, the lower pH can increase the potential difference between the anode and the cathode during micro-electrolysis, thereby promoting the production of Fe^{2+} and promoting the progress of the micro-electrolysis reaction. Fe^{2+}, as a catalyst for the Fenton reaction, can effectively participate in the degradation of organic matter [27]. When the pH is increased, there are three main reasons for the decrease in COD removal efficiency. First, the amount of Fe^{2+} produced is insufficient, that is, the amount of catalyst is insufficient, which will directly affect the Fenton degradation process. Second, the higher the pH, the easier it is to oxidize Fe^{2+} into Fe^{3+}, and the catalytic effect of Fe^{3+} is far less than Fe^{2+}, which further weakens the degradation of organic matter [28]. In addition, the •OH produced by H_2O_2 plays a role in degrading organic matter in Fenton process, while the higher pH will directly affect the production of •OH, which is extremely adverse to Fenton reaction. Redundant H_2O_2 will also be detected in the subsequent detection and interfere with the determination of COD [29].

In the parameter optimization experiment of ICME, COD removal efficiency at pH = 2 was slightly higher than that at pH = 3. In the parameter optimization experiment of ICME-H_2O_2, COD removal efficiency when pH is 2 is lower than that of pH = 3. This is mainly because when pH is 2, the amount of Fe^{2+} produced reaches supersaturated state, instead, H_2O_2 will be consumed to oxidize Fe^{2+} to Fe^{3+}. In conclusion, strict control of pH is crucial to the strengthening process, and the optimal pH was selected as 3.

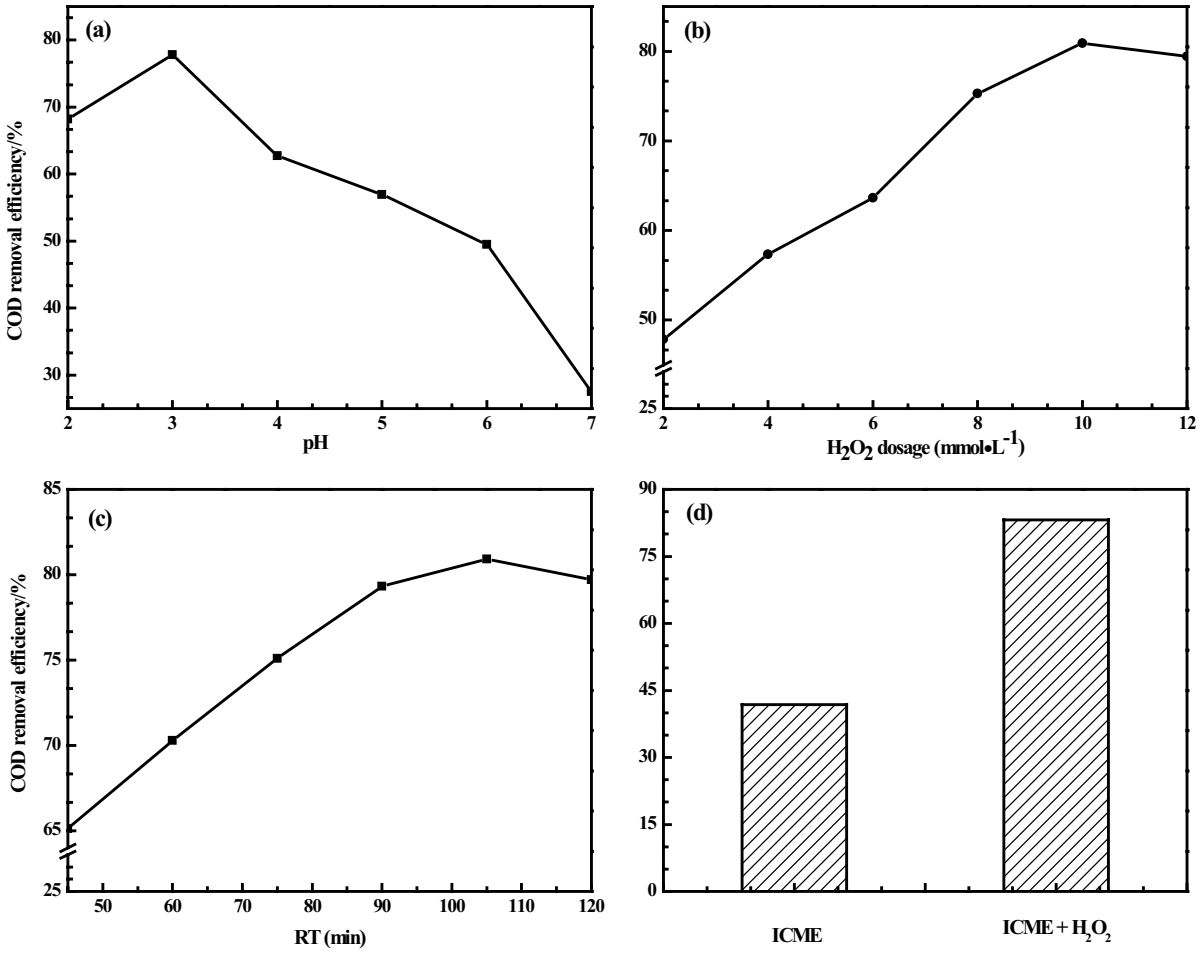

Fig. 3. Effects of (a) pH (iron dosage = 25 g/L, Fe/C = 1:2.5, RT = 90 min, H_2O_2 = 8 mmol/L), (b) H_2O_2 dosage (iron dosage = 25 g/L, Fe/C = 1:2.5, RT = 90 min, and pH = 3), (c) reaction time (iron dosage = 25 g/L, Fe/C = 1:2.5, H_2O_2 = 10 mmol/L, and pH = 3) on COD removal efficiency using ICME-H_2O_2, and (d) COD removal efficiency of different methods.

3.2.2. Effect of H_2O_2 dosage on COD removal efficiency

It can be seen from Fig. 3b, that with the increase of H_2O_2 dosage, the removal efficiency of COD also tends to increase gradually. When the dosage is 10 mmol/L, the removal efficiency reaches 80%, and then with the further increase of H_2O_2, the COD removal efficiency showed a decreasing trend.

When the amount of oxidant is insufficient in the early stage, COD is difficult to be effectively removed. The main effect is the subsequent coagulation and precipitation and the oxidation of H_2O_2 [30]. When the dosage is increasing, the amount of •OH in water is increasing, and the organic matter is gradually removed, and reaches a peak when the dosage is 10 mmol/L, indicating that the yield of •OH is the highest, mainly for oxidative decomposition of organic matter.

When the dosage is continuously increased, the excess •OH oxidizes Fe^{2+} to Fe^{3+} due to the •OH produced. As mentioned above, Fe^{3+} has the low catalytic capacity, which directly impedes the production of •OH and inhibits the degradation of organic matter [31]. Therefore, from the perspective of economic and processing effects, 10 mmol/L is selected as the optimum dosage.

3.2.3. Effect of reaction time on COD removal efficiency

Obtained curve is shown in Fig. 3c. Under the condition that the dosage and other conditions required for the reaction are satisfied, as the reaction time increases gradually, the COD removal efficiency also increases gradually, reaching a peak at 105 min, and the removal efficiency is 80%, which then shows a downward trend. It can be predicted that with the further increase of reaction time, COD removal efficiency will slowly decrease. According to the analysis, when the optimal removal efficiency is reached, the reaction time continues to increase, and the pH will increase further. It leads to the production and deposition of some flocs, which impedes the reaction. Moreover, the increased response time does not achieve the goal of increasing removal efficiency, and the capital expenditure will also increase. As can be seen from the figure, when the reaction time was 90 min, the removal efficiency was 79%. Therefore, 90 min should be selected.

3.2.4. Orthogonal test

In order to determine the optimal experimental conditions for the ICME-H_2O_2 system, orthogonal tests were carried out and the results are shown in Table S3. The results of orthogonal test are analyzed in Table S4. According to the value of R_X, the order of the influence of these factors on the treatment effect is as follows: pH > reaction time > concentration of H_2O_2. The best experimental parameters for the ICME-H_2O_2 are that pH 2.5, H_2O_2 dosage 9 mmol/L, and the reaction time is 100 min.

3.3. TOC and biodegradability evolution during ICME or ICME-H_2O_2 process

3.3.1. Comparison of the effects of ICME and ICME-H_2O_2

In order to compare the treatment effect of ICME and ICME-H_2O_2, the COD removal efficiency was compared under the best-operating conditions of the two processes.

Combined with Fig. 3d and Table 4, it can be seen that ICME has a certain effect on the removal of organic pollutants in BTEPM, and the treatment efficiency can reach about 41% while the ICME-H_2O_2 can reach about 81% under the optimal operating condition. It shows that adding H_2O_2 can increase the COD removal effect greatly of iron–carbon micro-electrolysis. Under the ICME-H_2O_2 process, the main role of •OH is for the advanced oxidation of organic matter, but it is undeniable that ICME also plays an important role in the degradation process. It can not only produce Fe^{2+}, but also promote the production of •OH, and also play a role in degrading organic matter or converting macromolecular organic matter into small molecular substances to some extent [32].

3.3.2. The variation of TOC and COD in ICME and ICME-H_2O_2 over time

In order to investigate the variation of TOC and COD with time in the process of ICME and ICME-H_2O_2, the TOC and COD were measured, and the experimental results are shown in Fig. 4a. It can be seen from the figure that in the process of ICME, both TOC and COD decrease slightly in the first 20 min. Then COD gradually decreased, while TOC was almost a horizontal line, indicating that the process of ICME had limited removal capacity for COD and TOC. In general, COD and TOC change in the same law.

In the ICME-H_2O_2 process, it can be seen from the figure that the trend of TOC and COD curve changes is consistent. Within 0–20 min, both TOC and COD are greatly reduced. After that, COD gradually decreases and tends to be stable, and TOC also tends to be stable. In the range of 80–100 min, it is almost parallel, showing good correlation. We can see that TOC removal was higher in ICME but COD removal was higher in ICME-H_2O_2, the reason needs further exploration.

3.3.3. Variation of BOD_5 in ICME and ICME-H_2O_2 over time

According to Fig. S1, in the ICME-H_2O_2, the value of BOD_5 gradually increases with the increase of time, and the

Table 4
Effluent water quality of different methods

Samples	pH	COD (mg/L)	SS (mg/L)	Color (mgPt/L)
BTEPM	6.5 ± 0.5	223 ± 10	39 ± 5	85 ± 5
ICME effluent	7.3 ± 0.5	129 ± 8	6 ± 3	5 ± 2
ICME-H_2O_2 effluent	7.5 ± 0.5	39 ± 6	5 ± 3	5 ± 2

value of BOD_5 reaches 23 mg/L at around 40 min, then tends to be gentle. Analysis shows that the gradual stability of BOD_5 is mainly due to the slow degradation of COD. Since the amount of oxidant H_2O_2 added in the initial reaction was a certain amount, the amount of •OH became less and less as time went on, and the value of BOD_5 tended to be saturated. With the gradual decrease of COD in the system, the ratio of BOD_5/COD becomes larger and larger, and the biodegradability becomes higher and higher. At 100 min, *B*/*C* reached 0.54, which greatly improved the biodegradability of wastewater. It can be predicted that with the stabilization of BOD_5 and COD, the biodegradability will also become stable.

According to Fig. S2, in the ICME, the value of BOD_5 gradually increases with time, and the value of BOD_5 reaches 34 mg/L at 60 min, and then tends to be gentle. According to the analysis, the removal efficiency of COD by ICME is limited. As the COD removal efficiency tends to be gentle, the value of BOD tends to be stable. The main reason is that with the progress of ICME, the rate of micro-electrolysis becomes slower and slower, and the pH value gradually increases, which causes poor degradation of pollutants in the system. With the gradual decrease of COD in the system, the ratio of *B*/*C* becomes larger and larger, and the biodegradability becomes higher and higher. At 100 min, *B*/*C* reached 0.24, which greatly improved the biodegradability of wastewater. In view of the limited removal effect of micro-electrolysis on the COD, the COD value is relatively high, although the *B*/*C* is greatly improved, the biodegradability after treatment is still not very ideal.

As shown in Fig. 4b, on the whole, BOD_5 of effluent from ICME-H_2O_2 is lower than that from ICME, but according to the value of *B*/*C*, the biodegradability of the effluent treated by ICME-H_2O_2 is significantly higher than that of the effluent treated by ICME. The effect of electrolysis on COD removal is limited, and the effluent COD value is still high. Although the effluent BOD value is higher, the *B*/*C* is still low.

3.4. Analysis of the mechanism of COD removal

3.4.1. Ultraviolet-visible spectroscopy of effluent from ICME and ICME-H_2O_2

In order to study the variation rule of organic matter under the optimal operating conditions of ICME and ICME-H_2O_2 process, the effluent was analyzed by ultraviolet-visible spectroscopy, and the absorbance wavelength curve is shown in Figs. 4c and d. When the reaction time increases

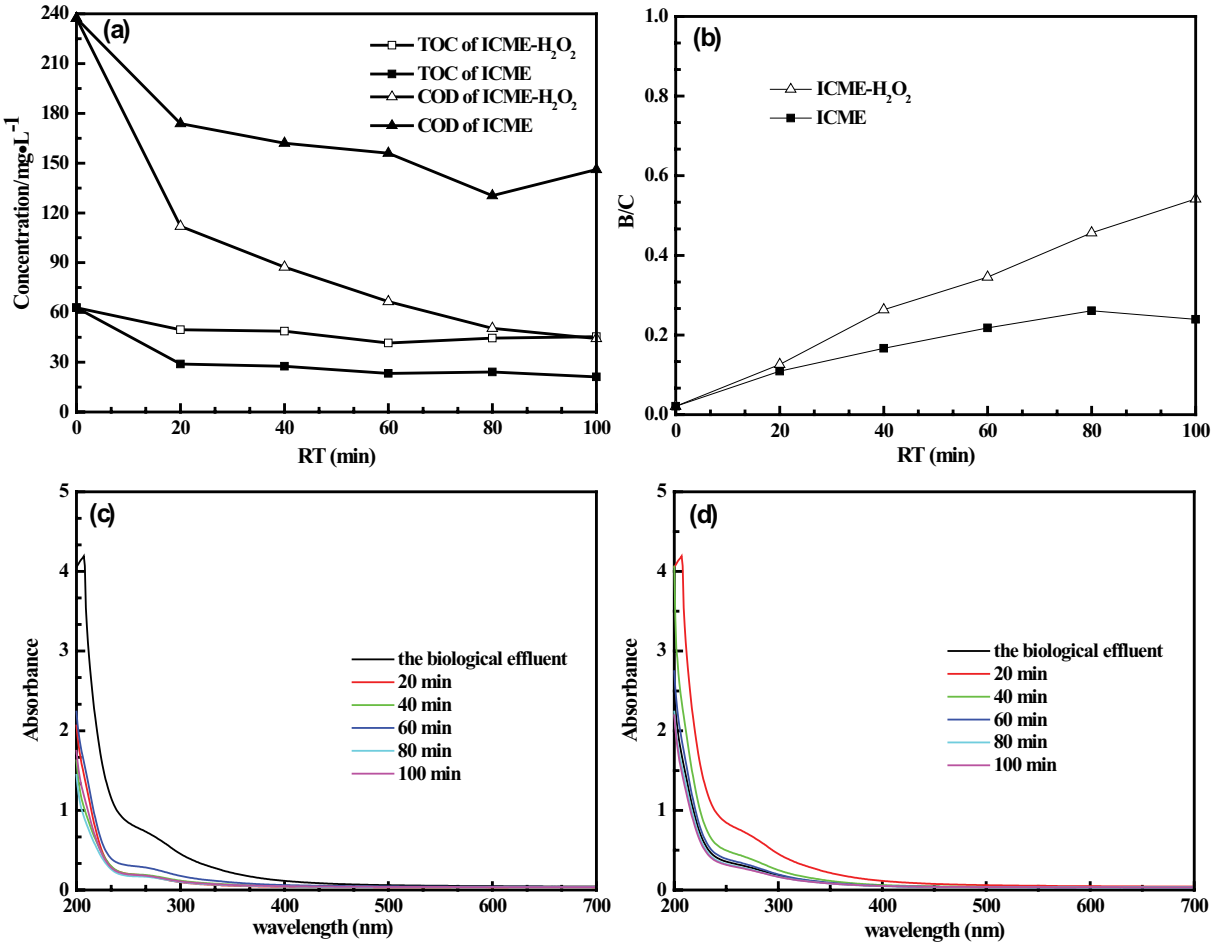

Fig. 4. (a) Evolution of TOC and COD content during ICME-H_2O_2 or ICME experiment, (b) biodegradability evolution along a ICME-H_2O_2 or ICME experiment, (c and d) full-band spectrum of a ICME-H_2O_2 (c) or ICME (d) process.

gradually, the height of the absorption peak gradually decreases, and the overall position of the curve gradually shifts downward, resulting in a blue shift, indicating that the organic matter content is gradually reduced [33], and the macromolecular substances are gradually degraded into small molecular substances, and the water quality is somewhat improvement. However, the curve of ICME has a small decrease, and the improvement of water quality is not as obvious as the ICME-H_2O_2 process, which is consistent with the test results of COD and TOC.

3.4.2. Degradation kinetics of ICME-H_2O_2

In order to study the degradation mechanism of ICME-H_2O_2, the kinetic experiment data were fitted with the zero-order reaction, double exponential, and second-order reaction kinetic models. The fitting results are demonstrated in Fig. S3. The correlation coefficients (R^2 = 0.999) of double exponential model are much higher than other kinetic models, indicating that the double exponential model has the best fitting effect. This may mean that the overall degradation of BTEPM in ICME-H_2O_2 system consists of two parallel pseudo-first-order processes with different degradation rates. However, because $k_{1,1}$ = 2.556 1/min, $k_{1,2}$ = 0.016 1/min, $k_{1,1}$ is much larger than $k_{1,2}$, it means that one of the reactions is insignificant, and the other pseudo-first-order degradation process is dominant [18].

3.4.3. Rule of iron salt change in ICME-H_2O_2

In order to reflect the change of iron in the reaction process more intuitively, the contents of total iron, Fe^{2+}, Fe^{3+} in the process were determined, as shown in Fig. 5a. In the 0–10 min stage, the detection content of Fe^{2+} is lower, while the content of Fe^{3+} shows a rising trend. The mechanism of Fenton reaction is as follows [34,35]:

$$Fe^{2+} + H_2O_2 \rightarrow Fe^{3+} + OH^- + {}^{\bullet}OH \quad (8)$$

$$Fe^{3+} + H_2O_2 \rightarrow Fe^{2+} + HO_2^{\bullet} + H^+ \quad (9)$$

$$Fe^{2+} + {}^{\bullet}OH \rightarrow Fe^{3+} + OH^- \quad (10)$$

$$Fe^{3+} + HO_2^{\bullet} \rightarrow Fe^{2+} + O_2 + H^+ \quad (11)$$

$$Fe^{2+} + HO_2^{\bullet} \rightarrow Fe^{3+} + HO_2^- \quad (12)$$

$${}^{\bullet}OH + H_2O_2 \rightarrow HO_2^{\bullet} + H_2O \quad (13)$$

The Fenton reaction is a chain reaction, and the beginning of the chain is that Fe^{2+} participates in the decomposition of H_2O_2 to produce $^{\bullet}OH$. It is indicated that in the combined process, a large amount of Fe^{2+} participates in the reaction of catalyzing H_2O_2 to produce $^{\bullet}OH$ in the first 10 min. Most of the H_2O_2 exists in the form of $^{\bullet}OH$ in water. Within 10–60 min, the total iron content showed a gentle upward trend, indicating that the electrode reaction was taking place in the system at this time, and organic matter was being effectively degraded, and COD was gradually decreasing. From 60 to 80 min, Fe^{2+} and total iron content began to increase, indicating that Fenton and Fenton-like reaction rates tended to slow down, and COD degradation rate began to decrease. Within 80–100 min, the overall trend began to slow down again, indicating that micro-electrolysis and Fenton reactions in the system began to become stable. As can be seen from Fig. 5a, with the continuous increase of reaction time, the total iron content tends to be stable, and Fe^{2+} tends to decrease. According to the analysis, the reaction in the system will consume H^+, and then the pH will increase [14], and Fe^{2+} will be oxidized to Fe^{3+}, the total iron finally stabilized at about 153 mg/L.

3.4.4. Variation law of H_2O_2 in ICME and ICME-H_2O_2

In order to explore the variation of H_2O_2 with time during the experiment, the concentration of H_2O_2 was measured,

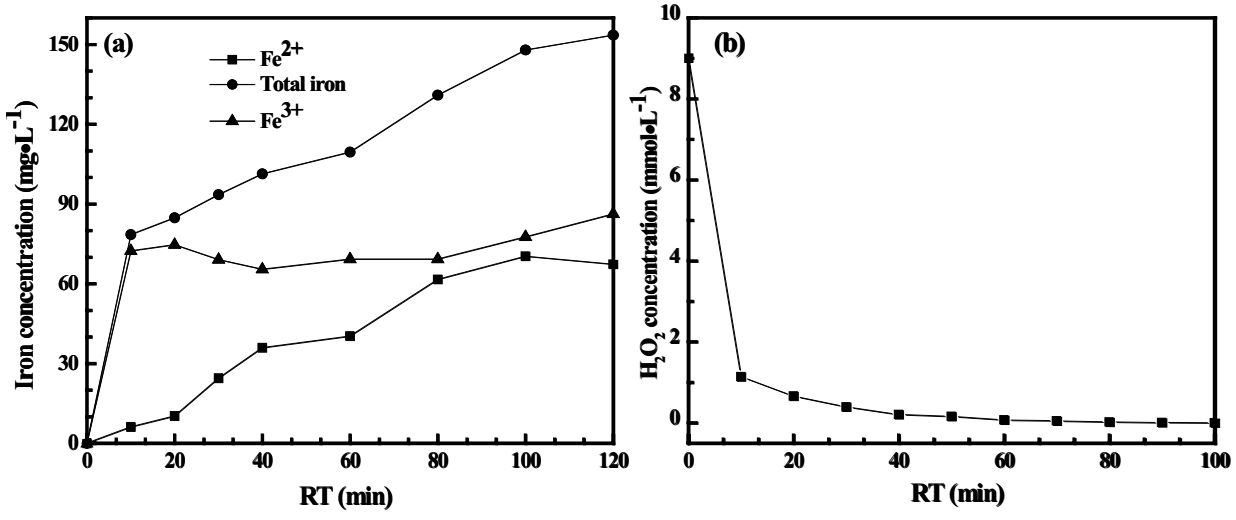

Fig. 5. Evolution of iron (a) and H_2O_2 (b) concentration during ICME-H_2O_2 process. (iron dosage = 25 g/L, Fe/C = 1:2.5, H_2O_2 = 9 mmol/L, and pH = 2.5).

and the curve is shown in Fig. 5b. Within 0–10 min, the content of H_2O_2 has a cliff-like decline, which is combined with the change of iron in each form in Fig. 5a. In the acidic environment, after the Fe^{2+} is produced, a large amount of H_2O_2 is decomposed into the form of •OH in the water. Its oxidation–reduction potential of 2.80 V is second only to fluorine [36], which can decompose a large amount of organic pollutants in water; then, the content of H_2O_2 gradually decreases, and the reaction is complete at about 100 min. At this time, there is basically no ability to continue to degrade organic matter in the system. The COD removal efficiency is the highest.

4. Conclusion

The optimum experimental conditions were explored by orthogonal tests. The optimum conditions for ICME is that the iron dosage is 25 g/L, the ratio of Fe/C is 1:2.5, pH is 2.5, reaction time is 90 min, and the optimum conditions for ICME-H_2O_2 is that pH is 2.5, the H_2O_2 dosage is 9 mmol/L, reaction time is 100 min. The COD removal efficiency of ICME and ICME-H_2O_2 can reach 42% and 81%, respectively. The addition of H_2O_2 can greatly improve the ability of micro-electrolysis system to remove pollutants. The biodegradability of wastewater after both processes has been improved, but the biodegradability of wastewater after ICME-H_2O_2 treatment has been improved more. The removal of COD in the ICME-H_2O_2 system mainly depends on the synergistic effect of •OH degradation and iron hydroxide flocculation. In a word, ICME-H_2O_2 can be used in the advanced treatment of papermaking wastewater.

References

[1] Z. Feng, H. Chen, H. Li, R. Yuan, F. Wang, Z. Chen, B. Zhou, Preparation, characterization, and application of magnetic activated carbon for treatment of biologically treated papermaking wastewater, Sci. Total Environ., 713 (2020) 136423.

[2] G. Vilardi, J.M. Ochando-Pulido, M. Stoller, N. Verdone, L. Di Palma, Fenton oxidation and chromium recovery from tannery wastewater by means of iron-based coated biomass as heterogeneous catalyst in fixed-bed columns, Chem. Eng. J., 351 (2018) 1–11.

[3] G. Vilardi, J. Rodríguez-Rodríguez, J.M. Ochando-Pulido, N. Verdone, A. Martinez-Ferez, L. Di Palma, Large laboratory-plant application for the treatment of a Tannery wastewater by Fenton oxidation: Fe(II) and nZVI catalysts comparison and kinetic modelling, Process Saf. Environ. Prot., 117 (2018) 629–638.

[4] G. Li, J. Yu, Y. Zhang, L. Gao, B. He, Study on treatment of wastewater from papermaking using Fenton oxidation, Adv. Mater. Res., 726–731 (2013) 1760–1763.

[5] L. Zhang, M. Wu, Y. Han, M. Liu, J. Niu, Structural parameter optimization for novel internal-loop iron–carbon micro-electrolysis reactors using computational fluid dynamics, Chin. J. Chem. Eng., 27 (2019) 737–744.

[6] M. Kamali, Z. Khodaparast, Review on recent developments on pulp and paper mill wastewater treatment, Ecotoxicol. Environ. Saf., 114 (2015) 326–342.

[7] D.S. Babu, V. Srivastava, P.V. Nidheesh, M.S. Kumar, Detoxification of water and wastewater by advanced oxidation processes, Sci. Total Environ., 696 (2019) 133961.

[8] B. Jiang, J. Zheng, X. Lu, Q. Liu, M. Wu, Z. Yan, S. Qiu, Q. Xue, Z. Wei, H. Xiao, M. Liu, Degradation of organic dye by pulsed discharge non-thermal plasma technology assisted with modified activated carbon fibers, Chem. Eng. J., 215–216 (2013) 969–978.

[9] Y.Z. Lin, M.Y. Liu, X.H. Liu, G.D. Wang, Pre-treatment of tin-plating wastewater from cold strip mill with H_2O_2-ferric/carbon, Iron Steel, 42 (2007) 79–81.

[10] Y. Chen, T. Lin, W. Chen, Enhanced removal of organic matter and typical disinfection byproduct precursors in combined iron–carbon micro electrolysis-UBAF process for drinking water pre-treatment, J. Environ. Sci., 78 (2019) 315–327.

[11] B. Yang, Y. Gao, D. Yan, H. Xu, J. Wang, Degradation characteristics of color Index direct blue 15 dye using iron-carbon micro-electrolysis coupled with H2O2, Int. J. Environ. Res. Public Health, 15 (2018) 15–23.

[12] K. Chanworrawoot, M. Hunsom, Treatment of wastewater from pulp and paper mill industry by electrochemical methods in membrane reactor, J. Environ. Manage., 113 (2012) 399–406.

[13] C. Ma, Z. Ran, Z. Yang, L. Wang, C. Wen, B. Zhao, H. Zhang, Efficient pretreatment of industrial estate wastewater for biodegradability enhancement using a micro-electrolysis-circulatory system, J. Environ. Manage., 250 (2019) 109492.

[14] Z. Yi, J. Xu, M. Chen, W. Li, J. Yao, H. Chen, F. Wang, Removal of uranium(VI) from aqueous solution using sponge iron, J. Radioanal. Nucl. Chem., 298 (2013) 955–961.

[15] C. Sun, L.I. Shao-Feng, C. Williams, H.C. Tao, Spectrophotometric determination of hydrogen peroxide in O_3/H_2O_2 advanced oxidation system with titanium oxalate, Chem. Eng. Process., 25 (2011) 27–31.

[16] S. Xia, R. Lin, X. Cui, J. Shan, The application of orthogonal test method in the parameters optimization of PEMFC under steady working condition, Int. J. Hydrogen Energy, 41 (2016) 11380–11390.

[17] R. Lin, X. Diao, T. Ma, S. Tang, L. Chen, D. Liu, Optimized microporous layer for improving polymer exchange membrane fuel cell performance using orthogonal test design, Appl. Energy, 254 (2019) 113714.

[18] F. Han, X. Ye, Q. Chen, H. Long, Y. Rao, The oxidative degradation of diclofenac using the activation of peroxymonosulfate by $BiFeO_3$ microspheres—kinetics, role of visible light and decay pathways, Sep. Purif. Technol., 232 (2020) 115967.

[19] X. Liu, J. Liu, J. Bi, F. Cao, Y. Ding, J. Peng, Effects of high pressure homogenization on physical stability and carotenoid degradation kinetics of carrot beverage during storage, J. Food Eng., 263 (2019) 63–69.

[20] M. Li, D. Zou, H. Zou, D. Fan, Degradation of nitrobenzene in simulated wastewater by iron–carbon micro-electrolysis packing, Environ. Technol., 33 (2011) 1761–1766.

[21] Y. Wang, Y. Liu, W. Fu, L. Chen, Y. Li, S. Wu, Treatment of actual dyeing wastewater by continuous iron-carbon micro-electrolysis process, Adv. Mater. Res., 838–841 (2013) 2395–2399.

[22] S. Lan, X. Wu, Y. Wang, Treatment of mid-stage pulping effluent using the combined process of microelectrolysis and Fenton oxidation-coagulation, Appl. Mech. Mater., 295–298 (2013) 2001–2010.

[23] H. Zhuang, S. Shan, C. Fang, Y. Song, X. Xue, Advanced treatment of paper mill wastewater using electro-fenton process with novel catalytic particle electrodes, BioResources, 13 (2018) 4175–4186.

[24] X. Zheng, M. Jin, X. Zhou, W. Chen, D. Lu, Y. Zhang, X. Shao, Enhanced removal mechanism of iron carbon micro-electrolysis constructed wetland on C, N, and P in salty permitted effluent of wastewater treatment plant, Sci. Total Environ., 649 (2019) 21–30.

[25] M. Panizza, G. Cerisola, Removal of organic pollutants from industrial wastewater by electrogenerated Fenton's reagent, Water Res., 35 (2001) 3987–3992.

[26] S. Giray, M. Morcali, S. Akarsu, C. Zıba, M. Dolaz, Comparison of classic Fenton with ultrasound Fenton processes on industrial textile wastewater, Sustainable Environ. Res., 28 (2018) 165–170.

[27] X. Wang, X. Gong, Q. Zhang, H. Du, Degradation mechanism of Direct Pink 12B treated by iron-carbon micro-electrolysis and Fenton reaction, J. Environ. Sci., 25 (2013) S63–S68.

[28] C. Huang, F. Peng, H.-J. Guo, C. Wang, M.-T. Luo, C. Zhao, L. Xiong, X.-F. Chen, X.-D. Chen, Efficient COD degradation of turpentine processing wastewater by combination of Fe–C

micro-electrolysis and Fenton treatment: long-term study and scale up, Chem. Eng. J., 351 (2018) 697–707.
[29] J. Zhao, S. Ye, Y.-y. Wang, X.-y. You, L.-y. Chai, Y.-d. Shu, Electrochemical degradation of acidified reed pulp black liquor with three-dimensional electrode reactor, J. Cent. South Univ., 22 (2015) 2945–2953.
[30] D. Pokhrel, T. Viraraghavan, Treatment of pulp and paper mill wastewater—a review, Sci. Total Environ., 333 (2004) 37–58.
[31] M. Malakootian, K. Kannan, M.A. Gharaghani, A. Dehdarirad, A. Nasiri, Y.D. Shahamat, H. Mahdizadeh, Removal of metronidazole from wastewater by Fe/charcoal micro electrolysis fluidized bed reactor, J. Environ. Chem. Eng., 7 (2019) 103457.
[32] L. Wang, Q. Yang, D. Wang, X. Li, G. Zeng, Z. Li, Y. Deng, J. Liu, K. Yi, Advanced landfill leachate treatment using iron-carbon microelectrolysis-Fenton process: process optimization and column experiments, J. Hazard. Mater., 318 (2016) 460–467.
[33] C. Zhang, M. Zhou, G. Ren, X. Yu, L. Ma, J. Yang, F. Yu, Heterogeneous electro-Fenton using modified iron–carbon as catalyst for 2,4-dichlorophenol degradation: influence factors, mechanism and degradation pathway, Water Res., 70 (2015) 414–424.
[34] H. He, D. Wu, Advanced oxidation treatment of papermaking wastewater by homogeneous Fenton reaction, Adv. Mater. Res., 726–731 (2013) 2510–2514.
[35] M.N. Morshed, N. Bouazizi, N. Behary, J. Guan, V. Nierstrasz, Stabilization of zero valent iron (Fe^0) on plasma/dendrimer functionalized polyester fabrics for Fenton-like removal of hazardous water pollutants, Chem. Eng. J., 374 (2019) 658–673.
[36] X. Xu, Y. Cheng, T. Zhang, F. Ji, X. Xu, Treatment of pharmaceutical wastewater using interior micro-electrolysis/ Fenton oxidation–coagulation and biological degradation, Chemosphere, 152 (2016) 23–30.

Supplementary information

Table S1
Design and result of ICME orthogonal test

Test number	Parameters				
	Iron scrap (g/L) (*A*)	Fe/C ratio (*B*)	pH (*C*)	RT (min) (*D*)	Removal efficiency (%)
1	15	1:1.5	2.5	80	34.53
2	15	1:2	3	90	26.52
3	15	1:2.5	3.5	100	34.67
4	20	1:1.5	3	100	31.49
5	20	1:2	3.5	80	23.20
6	20	1:2.5	2.5	90	40.47
7	25	1:1.5	3.5	90	34.39
8	25	1:2	2.5	100	32.60
9	25	1:2.5	3	80	37.29

Table S2
Range analysis calculation results of ICME orthogonal test

Parameters	Factors (*X*)			
	Iron scrap (g/L) (*A*)	Fe/C ratio (*B*)	pH (*C*)	RT (min) (*D*)
$\bar{K}_{X,1}$	31.91	33.47	35.87	31.67
$\bar{K}_{X,2}$	31.72	27.44	31.77	33.79
$\bar{K}_{X,3}$	34.76	35.91	30.75	32.92
R_X	3.04	8.47	5.12	2.12

Table S3
Design and result of ICME-H_2O_2 orthogonal test

Test number	Parameters			
	pH (*A*)	H_2O_2 (mmol/L) (*B*)	RT (min) (*C*)	Removal efficiency (%)
1	2.5	9	80	80.10
2	2.5	10	90	82.51
3	2.5	11	100	84.51
4	3	9	90	81.95
5	3	10	100	85.36
6	3	11	80	76.83
7	3.5	9	100	71.00
8	3.5	10	80	54.93
9	3.5	11	90	61.04

Table S4
Range analysis calculation results of ICME-H_2O_2 orthogonal test

Parameters	Factors (*X*)		
	pH (*A*)	H_2O_2 (mmol/L) (*B*)	RT (min) (*C*)
$\bar{K}_{X,1}$	82.37	77.68	70.62
$\bar{K}_{X,2}$	81.38	74.27	75.17
$\bar{K}_{X,3}$	62.32	74.13	80.29
R_X	20.05	3.55	9.67

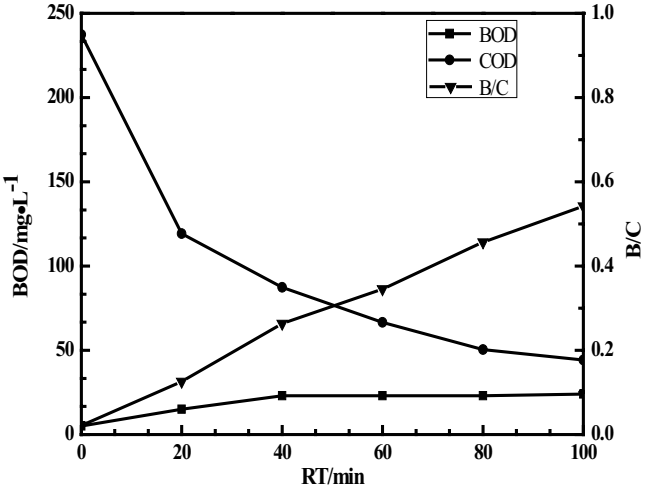

Fig. S1. Biodegradability of wastewater in ICME-H_2O_2 over time.

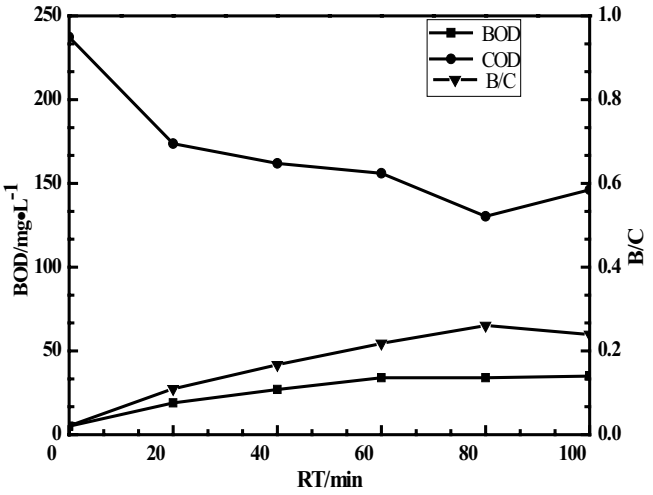

Fig. S2. Biodegradability of wastewater in ICME over time.

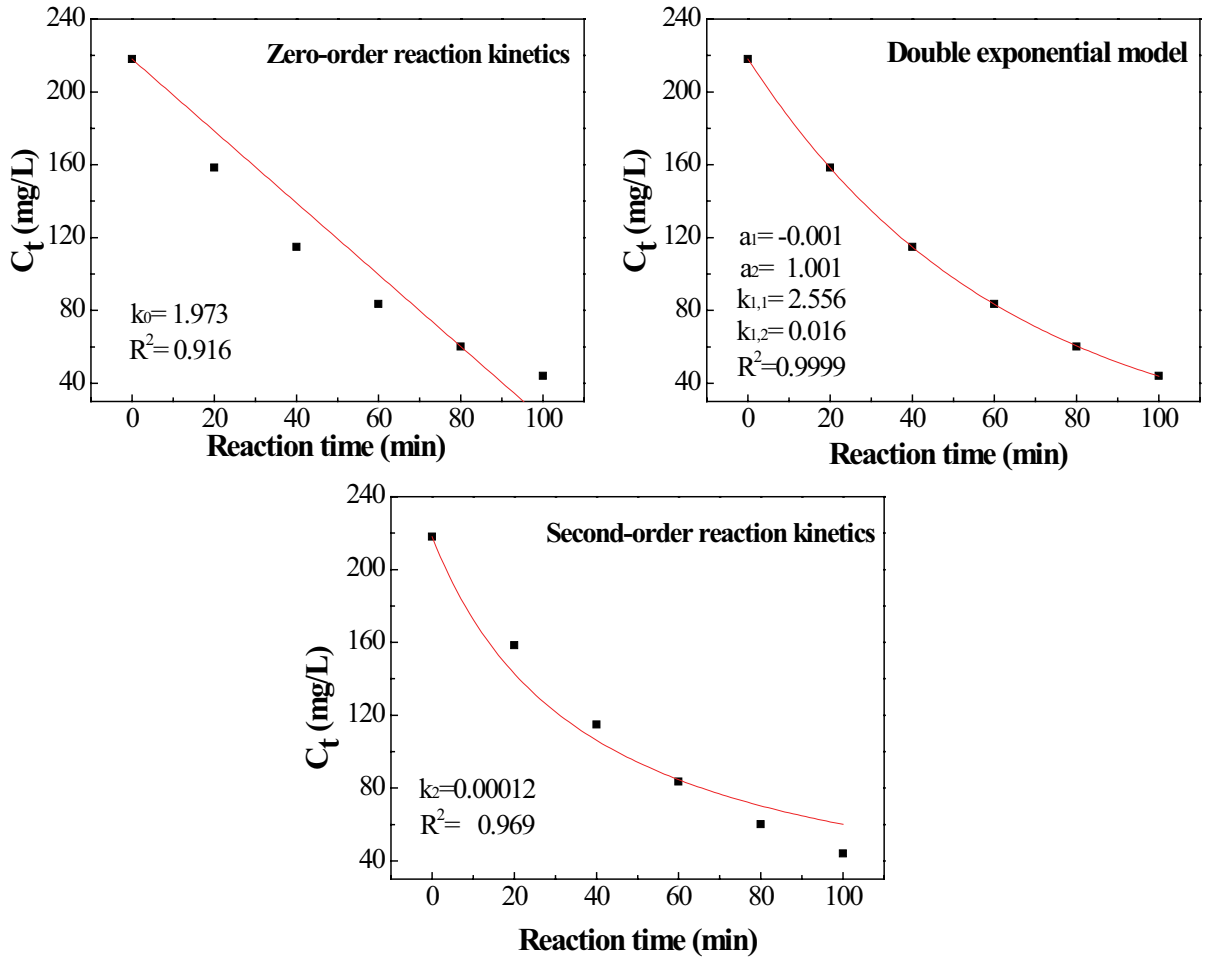

Fig. S3. Dynamic equation of ICME-H_2O_2.